Complex Spherical Micelles in A−B−C-Block Copolymer Melts

E. E. Dormidontova and A. R. Khokhlov*

Physics Department, Moscow State University, Moscow 117234, Russia

Received July 22, 1996; Revised Manuscript Received December 13, 1996[⊗]

ABSTRACT: Spherical micelles with complex inner structure in A−B−C-triblock copolymer melts with $N_A + N_B \ll N_C$ are considered in strong and superstrong segregation limits. It is assumed that blocks of polymer chain are different in length and strongly incompatible. One of the particular systems which we have in mind is a melt of B−C-block copolymer ($N_B \ll N_C$) with strongly associative A-groups at the end of B-block. In this case the formation of A-aggregates occurs inside the B-micelle, which is assumed in this paper to be spherical in shape. The inner structure of the B-micelle can be complicated. It is possible to distinguish between two principally different cases: (i) all A-blocks form a single aggregate at the center of the B-micelle and (ii) the A-aggregates form a certain structure inside the core of the B-micelle. It has been shown that, depending on the external parameters (such as temperature, monomer interaction parameters, block length, and monomer unit length), the characteristics of the B-micelle (aggregation number, size, position of A-aggregates inside the B-micelle) can be quite different. Thus, the size (aggregation number) of a polymer micelle with a single A-aggregate at the center is smaller than that for the B−C-diblock copolymer case. At the same time, for the polymer micelle with multi-A-aggregate inner structure the size and aggregation number of B-micelle are larger than that for B−C-diblock copolymer case. If the incompatibility of A- and B-blocks is much stronger than that for the B- and C-blocks, the polymer micelle with a single A-aggregate at the center is formed. Otherwise B-micelles have multi-A-aggregate inner structure. The presence of A-aggregates inside the B-micelle leads to stabilization of microphase separation between B and C in the system. For the system under consideration, the superstrong segregation regime for the central A-aggregate may be achieved for relatively small values of surface tension coefficients. In the superstrong segregation regime, the form of the A-aggregates is disklike. The regions of different structures of spherical B-micelles are represented on the diagram of states.

1. Introduction

Different polymer systems exhibiting microphase separation transition have been the object of intensive research during the last decades and this interest is continuously growing. Microdomain formation in diblock copolymer melts is well-studied, and the theory of microphase separation in these systems is developed to a large extent.[1−9] Microphase separation in more complicated polymer systems is the task for modern theoretical and experimental researches.

In this paper we will consider one of the more complicated polymer systems with microphase separation which is of significant experimental interest. Namely, we will consider the melt of A−B−C-triblock copolymers with blocks which are substantially different in lengths: $N_A + N_B \ll N_C$, (N_i is the number of monomer units in the block i, i = A, B, C). As might be expected from theory and experiments, if the B- and C-blocks in the system are incompatible, an ordered structure of spherical B-micelles in the medium of C-blocks is formed. Now, if a rather short A-block incompatible to the other blocks is attached to the end of the B-block, the B-micelle should have a complicated internal structure. The investigation of this structure and possible states of the system is the aim of the present paper.

Some of the experimental results for triblock copolymer systems are reported in refs 10−20. The main attention is directed to A−B−A-triblock copolymers.[11,12,15,16,19] A−B−C-triblock copolymers with comparable end-block lengths are also the object of intensive investigations.[13,14,17,18,20] Complex ordered structures with different morphologies have been observed experimentally for polystyrene-*block*-polybutadiene-*block*-poly(metyl methacrylate) (PS-*b*-PB-*b*-PMMA),[13,18,20] as well as for isoprene−styrene−2-vinylpyridine copolymers.[17] Variation in the length of the central block changes the type and morphology of the ordered structures.

The experimental triblock copolymer system which is most close to the case under consideration in the present paper was considered recently in ref 10, where the melt of polystyrene−polyisoprene (PS−PI) chains with ω-functionalized groups at the end have been studied. Here the role of a short A-block is played by strongly associating ω-functionalized groups (zwitteronic groups). The specific features of the ordered structures for the polymer melts have been studied in ref 10 by small-angle X-ray scattering (SAXS), rheology, and dielectric spectroscopy measurements. It has been found that the presence of ω-functionalized groups leads to stabilization of the ordered structures and that formation of the multiplets occurs inside the PS-micelle. The temperature dependence of intensity SAXS profiles has been obtained as well. In the present paper we will pay special attention to the analysis of the specific features of the ordered spherical micellar structures of triblock copolymer melt with short A-block. In spite of the difference in the shape of the micelles (for the polymer system of ref 10 the fraction of PS-block is 30%, which leads to the cylindrical shape of the PS-micelle in contrast to the present case), the basic features of behavior of both polymer systems are similar. So, below we will compare (at least qualitatively) our results with those of ref 10.

Theoretical analysis for triblock copolymer systems have also been performed[20−24] Theoretical calculations[20−23] have been performed in the strong segregation limit and are devoted to study of the ordered structures experimentally observed in symmetric triblock copolymers.[13,18,20,17] Since the triblock copolymer systems are more complicated in comparison with diblock copoly-

[⊗] Abstract published in *Advance ACS Abstracts,* February 1, 1997.

S0024-9297(96)01076-5 CCC: $14.00 © 1997 American Chemical Society

mers, theoretical calculations are more formidable and as a result this field of analysis is not so developed as for the diblock copolymer case. In the present research we intend to study specifically strongly asymmetric triblock copolymer systems.

The strongly associating A-blocks (or A-groups) will form aggregates inside the B-micelles which are analogous to the multiplets in ionomer polymer systems.[25−30] The statistical theory of such multiplets has been recently developed in refs 31−33 using the analogy with the "parent" block copolymer system. We adopt this approach in the present paper as well.

The complex structure of the B-micelle core influences the characteristics of the B-micelle (cf. also the experimental results of ref 10). We will assume below the spherical shape of the B-micelle; however, the size and internal structure will be defined from the conditions of thermodynamic equilibrium.

The present paper is organized as follows. In the next section the main ideas of the model are presented. In section 3 the different structures of B-micelle with spherical A-aggregates inside are considered. Section 4 is devoted to B-micelles with disklike A-aggregates. The different regimes of behavior of spherical B-micelle are summarized in section 5, where the diagram of states is presented. Lastly, section 6 contains the concluding remarks.

2. The Model

Let us consider the block copolymer melt. Each block copolymer chain consists of three blocks, A, B, and C. We suppose that the lengths of the blocks are different: the length of block C is much larger than the joint length of B- and A-blocks, i.e. $N_C \gg N_B + N_A$. All blocks A, B, and C are incompatible. Since the blocks are incompatible and the fraction of A- and B-blocks in the polymer system is small enough, we will assume that B-micelles have a spherical form, and blocks A and B are inside the core of this micelle (i.e. the incompatibility of A- and C-blocks is so strong that these blocks prefer to have no contact). In this polymer system two different types of separation (between A−B- and B−C-blocks) can take place. Since A-block is attached to B-block, which is incompatible with C, the formation of A-aggregates occurs inside the B-micelle. The form and distribution of A-aggregates depend on the lengths of the blocks, the temperature, and other parameters of the system. To describe the structure of A-aggregates inside the large B-micelle, let us consider the free energy of the ordered structure of spherical micelles. The free energy of the polymer system can be written in the form

$$F = F_{core} + F_{sur} + F_{corona} \tag{1}$$

where F_{core} is the free energy of the polymer blocks forming the core of the B-micelle, F_{sur} is the surface free energy for the B-micelles, and F_{corona} is the free energy connected with C-block extension in the corona region.

The difference between the structure of the spherical micelles under consideration and that for B−C-diblock copolymers is in the more complex structure of the B-micelle core. The contributions F_{sur}, and F_{corona} to the free energy (eq 1) are similar to the ones for the diblock copolymer case. The surface free energy for the B-micelles per one chain forming the micelle can be written in the form:[7,31]

$$F_{sur} = 4\pi\gamma_{BC}R_B^2/Q_B \tag{2}$$

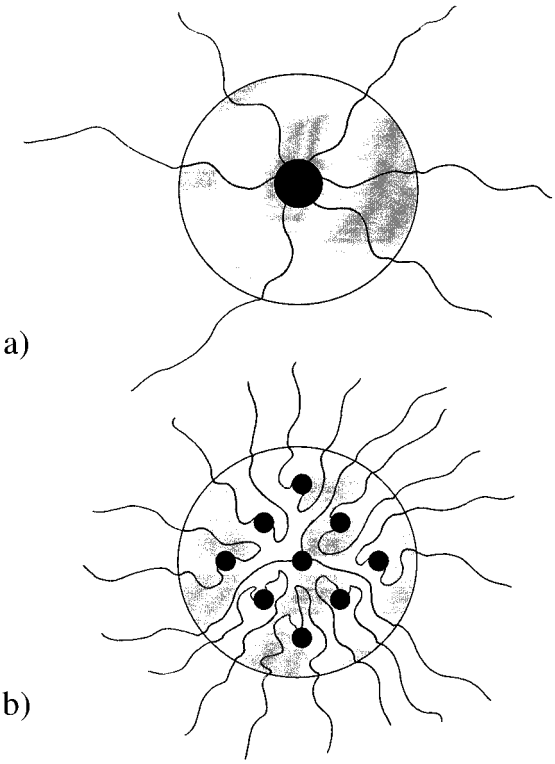

Figure 1. Schematic picture of two possible structures of a B-micelle with spherical A-aggregates: (a) a single A-aggregate at the centre of the B-micelle and (b) several A-aggregates inside the core of the B-micelle.

where R_B is the radius of the the B-micelle, Q_B is the total aggregation number of the B-micelle (i.e. the number of B-blocks forming the micelle), and γ_{BC} is the surface tension coefficient. The surface tension coefficient γ_{BC} is connected with the Flory−Huggins B−C monomer interaction parameter χ_{BC}:

$$\gamma_{BC} \simeq \frac{kT}{l^2}\sqrt{\chi_{BC}} \tag{3}$$

where l is the characteristic size of a monomer unit. The free energy F_{corona} (per chain) connected with the stretching of C-chains in the corona region of the B-micelle is the same as for a diblock copolymer micelle[7]

$$F_{corona} = kT\frac{3}{8\pi}\frac{\nu_C}{l_C^2}\frac{Q_B}{R_B} \tag{4}$$

where ν_i and l_i are the volume of a monomer unit and the statistical length of i-block (i = A, B, C).

Possible structures of a B-micelle are shown in Figure 1. The inner structure of the core of the B-micelle can be different (cf. parts a and b of Figure 1). The formation of A-aggregates (multiplets) occurs inside the core of the B-micelle. There are two different possibilities: a single A-aggregate inside the B-micelle (Figure 1a) or multiple A-aggregates within the B-micelle (Figure 1b).

To analyze the structure of A-aggregates inside the core of a B-micelle, let us consider qualitatively the possible distribution of A-blocks near the center of the core (Figure 2). Let us consider two possibilities: (i) several A-blocks are terminated at the center of the B-micelle (Figure 2a) (ii) there are no A-blocks at the center (Figure 2b). It is easy to show that the first possibility is thermodynamically preferable. Indeed, even if there are no A-blocks at the center, the central

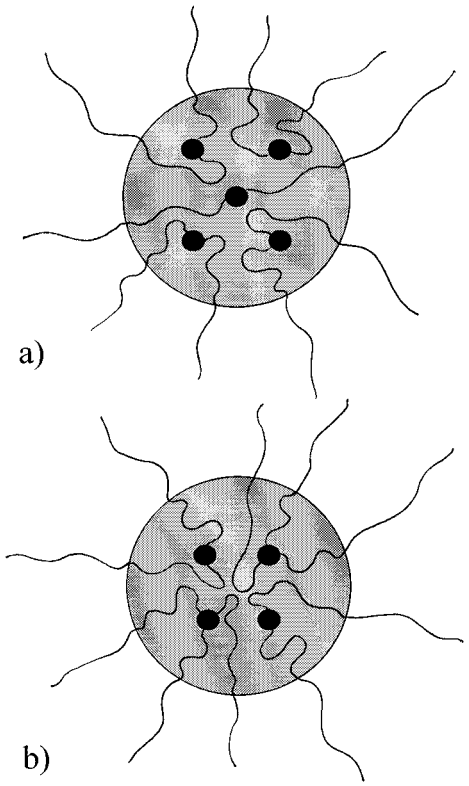

Figure 2. Possible conformation of polymer chains near the centre of a B-micelle: (a) there is an A-aggregate at the center and (b) the central aggregate is absent.

region of the B-micelle cannot be empty in a dense polymer system. Then this region should be filled by B-monomer units; this leads to an additional strong extension of the corresponding B-chains. On the other hand, there is no energy gain connected with pushing the A-aggregate out of the center of the micelle. These simple qualitative arguments lead us to the conclusion that in any case there is an A-aggregate at the center of a B-micelle. To obtain the expression for the free energy of the B-micellar core (F_{core}), let us consider in more detail the inner structure of a B-micelle. As we have seen above, there is an A-aggregate at the center of the micelle. Let us denote the radius of this central aggregate as R_0 and its aggregation number as Q_0. We will suppose in our simplest version of the theory that all other satellite A-aggregates are identical, with a radius of R_A and an aggregation number of Q_A. The size, form, and aggregation number of the central A-aggregate can be different or similar to ones of satellite A-aggregates. The equilibrium characteristics of central and satellite aggregates are to be determined from the minimum condition of the free energy of the system (eq 1).

It is easy to see that this model of the inner structure of B-micelles includes both cases shown in Figure 1. When all A-blocks form one aggregate at the center of the B-micelle, there are no satellite aggregates and R_A and Q_A are equal to zero.

In the framework of our model, the free energy per chain (F_{core}) can be written in the form

$$F_{core} = F^0_{core} + F^0_{sur} + F^A + F^B \qquad (5)$$

where F^0_{core} and F^0_{sur} are the free energy (per block copolymer chain) of the core and surface free energy for the central A-aggregate; F^A is the free energy of the system of satellite A-aggregates; F^B is the free energy of the B-block extension in the region between the surface of the central A-aggregate and the surface of the B-micelle core. The contributions F^0_{core} and F^0_{sur} to the free energy (eq 5) can be represented in the usual form (cf. refs 7 and 31):

$$F^0_{core} + F^0_{sur} = \left[kT\frac{3\pi^2}{80}\frac{{R_0}^2}{N_A {l_A}^2} + 4\pi {R_0}^2\frac{\gamma_{AB}}{Q_0}\right]\frac{Q_0}{Q_B} \qquad (6)$$

In eq 6 the expression in brackets corresponds to the contributions from the chain extension inside the core of the central A-aggregate and surface tension energy. To obtain the free energy per chain, we must multiply the expression in brackets by a factor of Q_0/Q_B, since this is the fraction of polymer chains forming the central aggregate.

The contribution F^A consists of three terms corresponding to the surface energy, the free energy of A-block extension inside the core, and the free energy of B-block extension in the corona of the satellite A-aggregates (cf. ref 31). It is convenient to divide the contribution of the free energy of B-blocks extension to F_{core} (eq 5) into two parts. The free energy of B-block extension in the regions near the surfaces of satellite A-aggregates is incorporated in the free energy of satellite A-aggregates, F^A. While it is convenient to consider the free energy of B-block extension in the remaining space of the core of the B-micelle as a separate contribution, F^B, to the free energy (eq 5). The free energy of B-chain extension in the corona of the central A-aggregate will also be taken into account in F^B. To obtain the free energy F^A per chain, the terms corresponding to the free energy of satellite A-aggregates are to be multiplied by the fraction of chains forming noncentral A-aggregates, i.e. by $1 - Q_0/Q_B$. As a result, the free energy F^A has the form

$$F^A = \left[4\pi {R_A}^2\frac{\gamma_{AB}}{Q_A} + kT\left(\frac{3\pi^2}{80} + \frac{1}{2}\right)\frac{{R_A}^2}{N_A {l_A}^2}\right]\left(1 - \frac{Q_0}{Q_B}\right) \qquad (7)$$

To calculate the contribution F^B to the free energy (eq 5) connected with the extension of B-blocks in the core of the micelle, let us consider in more detail the structure of the B-micelle. As has been mentioned above, there is an A-aggregate at the center of a B-micelle. B-blocks starting from the central A-aggregate are radially extended. The conformation of other B-blocks is more complicated. All B-blocks are radially stretched near the B−C-junction points, i.e. near the surface of the B-micellar core. But these B-blocks attaching to the surface of the B-micelle core terminate in different A-aggregates. The exact microscopic description of the behavior of all B-chains inside the core should be very cumbersome, and probably a very detailed description is beyond the current level of treatment of the model.

To obtain the expression for the elastic free energy F^B, we will use the electrostatic analogy[7,32] between the polymer chain conformations near surfaces and electric field lines near charged surfaces. In the framework of this analogy, the average vector connecting neighboring monomer units along the chain (dr/dn) (where $r(n)$ is the average distance of the n-th monomer unit of the chain from the surface) corresponds to the electric field, E. The aggregation numbers of the micelles correspond to the charges. The energy of the block extension is proportional in this approach to the electrostatic energy $W = 1/8\pi \int E^2\, d^3r$. Indeed for the free energy (per chain) of block extension it is possible to write the following

expression:

$$F = kT\frac{1}{Q}CW \tag{8}$$

where W is the electrostatic energy of the corresponding region and C is the polymer/electrostatic proportionality constant[32]

$$C = \frac{3}{4\pi}\frac{v}{l^2}$$

where v and l are the volume of monomer unit and statistical length of the chain. For example, for the C-block extension in the corona region we can obtain from eq 8 the following expression

$$F_{\text{corona}} = kT\frac{1}{Q_B}CW = kT\frac{1}{Q_B}C\frac{1}{2}\frac{{Q_B}^2}{R_B}$$

which coincides with eq 4.

The free energy of B-block extension (F^B) in the spherical layer between the surface of the central aggregate and the surface of B-micelle is calculated in the Appendix. The final expression for the free energy F^B has the form (eq A3)

$$F^B \simeq kT\frac{3}{8\pi}\frac{v_B}{{l_B}^2}\left\{\frac{{Q_0}^2}{Q_B}\frac{1}{R_0} + \frac{Q_0}{Q_B}\frac{(Q_B - Q_0)}{R_B} + \frac{1}{5}\frac{(Q_B - Q_0)^2}{Q_B R_B}\right\} \tag{9}$$

For the case $Q_0 = Q_B$, i.e. when there is only one A-aggregate at the center of the B-micelle (Figure 1a), the expression for the free energy F^B

takes the form

$$F^B \simeq kT\frac{3}{8\pi}\frac{v_B}{{l_B}^2}Q_B\frac{1}{R_0} \tag{10}$$

This expression (eq 10) can be easily obtained by a different method, used in refs 7 and 31.

Another limit $Q_0 \to 0$, corresponding to the case of an ordinary B−C-diblock copolymer melt, leads to the following expression for the free energy of B-block extension in the core of the micelle

$$F^B \simeq \text{const}\frac{{R_B}^2}{N_B{l_B}^2}kT$$

as it should.[7,31]

Now, when we have the expressions for all contributions to the free energy (eq 1) we can analyze the expression for the full free energy.

3. Spherical A-Aggregates inside the B-Micelle

In the previous section we have obtained the free energy for the model assuming that all A-aggregates inside the core of a B-micelle have a spherical form. As we will see below, such a situation is not always true. But in the present section we will limit ourselves to the consideration of only spherical A-aggregates.

Taking into account the relations between aggregation numbers (Q_i), volumes (V_i), and radii (R_i) of the micelles,

$$Q_B = \frac{V_B}{N_B v_B + N_A v_A} = \frac{4\pi}{3}\frac{{R_B}^3}{N_B v_B + N_A v_A}$$

$$Q_0 = \frac{V_0}{N_A v_A} = \frac{4\pi}{3}\frac{{R_0}^3}{N_A v_A} \qquad Q_A = \frac{V_A}{N_A v_A} = \frac{4\pi}{3}\frac{{R_A}^3}{N_A v_A} \tag{11}$$

the free energy F (eq 1) can be represented as a function of three variables, for instance, radii R_A, R_B, and R_0. When we calculated the expression for the free energy F^B, we did not make any assumptions about the size of the central aggregate. Simple analysis of the free energy F (eq 1) allows us to come to the conclusion that the free energy of the polymer system with $Q_0 = Q_A$ ($R_0 = R_A$) is always lower than for the case $Q_0 \neq Q_A$. It means that the inner structure of a B-micelle with identical A-aggregates is more favorable than for the case $Q_0 \neq Q_A$. Probably, a difference in the size of central and satellite aggregates can leads to extra stretching of B-chains near the center of the core. So, we can consider all A-aggregates to be identical. This result leads to some simplification in the form of the expression for the free energy:

$$\frac{F}{kT} = \left(\frac{1}{2} + \frac{3\pi^2}{80}\frac{v_A{l_B}^2}{v_B{l_A}^2}\right)\frac{{R_A}^2 v_B}{N_A{l_B}^2 v_A} + 3\frac{N_A v_A}{R_A}\frac{\gamma_{AB}}{kT} + \frac{1}{2}\frac{v_B}{{l_B}^2}\frac{1}{N_A v_A}\frac{{R_A}^3}{R_B}\left[1 - \left(\frac{R_A}{R_B}\right)^3\left(1 + \frac{N_B v_B}{N_A v_A}\right)\right] + \frac{1}{10}\frac{v_B}{{l_B}^2}\frac{{R_B}^2}{(N_B v_B + N_A v_A)}\left[1 - \left(\frac{R_A}{R_B}\right)^3\left(1 + \frac{N_B v_B}{N_A v_A}\right)\right]^2 + 3\frac{(N_B v_B + N_A v_A)}{R_B}\frac{\gamma_{BC}}{kT} + \frac{1}{2}\frac{{R_B}^2 v_C}{(N_B v_B + N_A v_A){l_C}^2} \tag{12}$$

The free energy (eq 12) depends on two variables, R_A and R_B. But there is a case when these two variables are not independent. This is the case of a single A-aggregate at the center of the B-micelle.

3.1. Single A-Aggregate at the Center of the B-Micelle. If all A-blocks inside the core of the B-micelle form one aggregate at the center, i.e. $Q_A = Q_B \equiv Q$, then the variables R_B and R_A are connected via the relation

$$\frac{R_B}{R_A} = \left(1 + \frac{N_B v_B}{N_A v_A}\right)^{1/3} \tag{13}$$

The free energy (eq 12) depends now only on one variable, e.g. R_A:

$$\frac{F}{kT} = \frac{1}{2}\left[1 + \frac{3\pi^2}{40}\frac{v_A{l_B}^2}{v_B{l_A}^2} + \frac{v_C{l_B}^2}{v_B{l_C}^2}\left(\frac{N_A v_A}{N_A v_A + N_B v_B}\right)^{1/3}\right] \times \frac{{R_A}^2 v_B}{N_A{l_B}^2 v_A} + 3\frac{N_A v_A}{R_A}\left\{\frac{\gamma_{AB}}{kT} + \left(1 + \frac{N_B v_B}{N_A v_A}\right)^{2/3}\frac{\gamma_{BC}}{kT}\right\} \tag{14}$$

The expression (14) for the free energy has a similar form as for the diblock copolymer case (see refs 7 and 31). The complex structure of the B-micelle results in the presence of the last terms in the square and curly

brackets of eq 14. The expression in the curly brackets can be interpreted as an effective surface tension coefficient [$\gamma_{eff}/(kT)$]:

$$\frac{\gamma_{eff}}{kT} = \frac{\gamma_{AB}}{kT} + \left(1 + \frac{N_B v_B}{N_A v_A}\right)^{2/3} \frac{\gamma_{BC}}{kT} \qquad (15)$$

The presence of the tension on the B−C-surface leads to a significant increase in the effective tension γ_{eff} and to an increase of the size of a central aggregate in comparison with the micelles in the melt of A−B-copolymers. The physical reason for this is connected with the fact that the distribution of A-blocks inside the B-micelle is nonuniform. Most of the A-blocks concentrate around the center of the micelle, even in the absence of the A−B-repulsion. On the other hand, in the A−B-copolymer melt, the distribution of the A-blocks in the absence of A−B-repulsion is uniform. To form a large A-aggregate, A-blocks should first gather in some region. The inhomogeneous distribution of A-blocks makes this process easier for the present case and serves as the additional factor for the formation of a larger A-aggregate in the center of the B-micelle.

Minimization of the free energy (eq 14) leads to the following expressions for the radii R_A and R_B and aggregation number Q:

$$R_A = \left[3(N_A v_A)^2 \frac{\gamma_{eff}}{kT} \frac{l_B^2}{v_B}\right]^{1/3} \qquad (16)$$

$$Q = \frac{4\pi N_A v_A}{S} \frac{\gamma_{eff}}{kT} \frac{l_B^2}{v_B} \qquad (17)$$

$$R_B = \left[\frac{3N_A v_A (N_A v_A + N_B v_B)}{S} \frac{\gamma_{eff}}{kT} \frac{l_B^2}{v_B}\right]^{1/3} \qquad (18)$$

where S is the expression in the square brackets of eq 14, i.e.

$$S = 1 + \frac{3\pi^2}{40} \frac{v_A l_B^2}{v_B l_A^2} + \frac{v_C l_B^2}{v_B l_C^2} \left(\frac{N_A v_A}{N_A v_A + N_B v_B}\right)^{1/3}$$

A comparison of the radius of A-aggregate (R_A) with that for the case of A−B-block copolymer (see e.g. refs 7, 31, and 33) shows that for the present case the A-aggregate is much larger ($R_A \gg R_{AB}$, $Q \gg Q_{AB}$). For the diblock copolymer case

$$R_{AB} \sim 3^{1/3} \frac{(N_A v_A)^{2/3} l_B^{2/3}}{v_B^{1/3} S_{AB}^{1/3}} \left(\frac{\gamma_{AB}}{kT}\right)^{1/3}$$

where

$$S_{AB} = 1 + \frac{3\pi^2}{40} \frac{v_A l_B^2}{v_B l_A^2}$$

This effect was already explained above. On the other hand, the size of the B-micelle (R_B) is smaller than for the B−C-diblock copolymer melts. This is apparently connected with the additional extension of the B-chains emanating from the A-aggregate.

The average distance between two B-micelles, λ_B, can be estimated as

$$\lambda_B \simeq (Q N_C v_C)^{1/3} \simeq \left[N_C v_C \frac{N_A v_A}{S} \frac{\gamma_{eff}}{kT} \frac{l_B^2}{v_B}\right]^{1/3} \qquad (19)$$

Since the aggregation number of the B-micelle (Q_B) is smaller than for the B−C-diblock copolymer case, the value of λ_B is smaller as well.[7]

As has been shown in ref 31, for extremely strong repulsion between the blocks, a new regime of behavior can be realized for block copolymers. This regime was called the superstrong segregation regime. The appearance of this regime is mainly connected with connectivity restrictions. Indeed, the size of the A-aggregate increases with the increase of A−B-incompatibility and at some stage the radius of the A-aggregate becomes about $N_A l_A$. (We will assume in this paper that all the chains are flexible and disregard the difference between statistical Kuhn segment length l_i, i = A, B, C, and the size of monomer units along the chain.) It is evident that a further increase of the size of a spherical A-aggregate is impossible. As a result, the form of the A-aggregate is transformed. In ref 32 it was shown that in the superstrong segregation regime A-aggregates should have a nonspherical form. Another reason leading to a transformation of the A-aggregate form (i.e. the transition to superstrong segregation regime) is the aggregate surface restriction. If the surface of the A-aggregate is completely covered by A−B-junction points, then the form of the aggregate should change. Both these reasons lead to similar requirements for the transition to the superstrong segregation limit. For the present case this condition is

$$\frac{\gamma_{eff}}{kT}\Big|_{ss} \equiv \left(\frac{\gamma_{AB}}{kT} + \left(1 + \frac{N_B v_B}{N_A v_A}\right)^{2/3} \frac{\gamma_{BC}}{kT}\right)\Big|_{ss} \geq \frac{N_A l_A^3 v_B}{v_A^2 l_B^2} S \qquad (20)$$

From the consideration above we have seen that the structure of the complex micelle depends on the effective surface tension γ_{eff}/kT (eq 15). Therefore, the superstrong segregation regime can be achieved more easily than for the ionomer case.[31] If

$$\frac{\gamma_{eff}}{kT} \simeq \frac{N_A l_A^3 v_B}{v_A^2 l_B^2} S$$

the main characteristics of the B-micelle structure turn out to be

$$R_A^{ss} \simeq N_A l_A \qquad R_B^{ss} \simeq \left(1 + \frac{N_B v_B}{N_A v_A}\right)^{1/3} N_A l_A \qquad (21)$$

$$Q^{ss} \simeq N_A^2 \frac{l_A^3}{v_A} \qquad \lambda_B^{ss} \simeq N_A^{2/3} N_C^{1/3} l_A \left(\frac{v_C}{v_A}\right)^{1/3}$$

where the superscript "ss" refers to the superstrong segregation regime.

Therefore, we conclude that for this case the superstrong segregation regime can be reached even for moderate values of incompatibility parameters, $\gamma_{eff}/(kT) \sim 1$, $\gamma_{BC}/(kT) \sim 1$, if the value of N_B is high enough. However, below we will see that in these cases B-micelles having more than one aggregate at the micelle center are more thermodynamically favorable. Further increase of $\gamma_{AB}/(kT)$ [$\gamma_{eff}/(kT)$] leads to a transformation of the A-aggregate form. As has been shown in ref 32, the more preferable form of an A-aggregate is disklike (Figure 3a). The structure of the complex B-micelle in

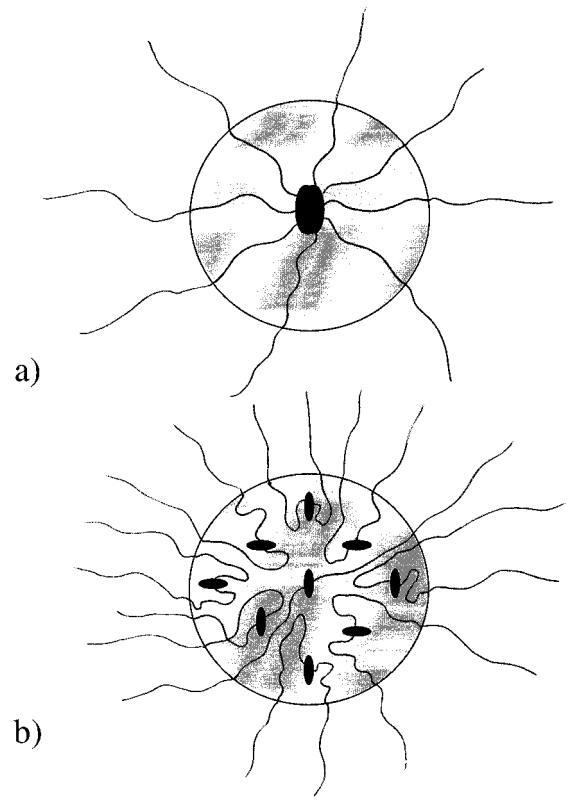

Figure 3. Schematic picture of possible structures of a B-micelle with disklike A-aggregates: (a) a single A-aggregate at the center of the B-micelle and (b) several A-aggregates inside the core of the B-micelle.

the superstrong segregation regime, when the central A-aggregate has a disklike form, will be considered in section 4.

3.2. Several A-Aggregates inside the Core of the B-Micelle. For the case of several A-aggregates inside the B-micelle core the values R_A and R_B are independent. Minimization of the free energy (eq 12) with respect to these variables leads to the following results

$$R_A \simeq R_A^0\left\{1 - \frac{3}{10}\frac{1}{S_1}\frac{R_A^0}{R_B^0}\left(1 - \frac{8}{3}\left(\frac{R_A^0}{R_B^0}\right)^3\left(1 + \frac{N_B v_B}{N_A v_B}\right)\right)\right\} \quad (22)$$

$$R_B \simeq R_B^0\left\{1 - \frac{8}{15}\left(\frac{R_A^0}{R_B^0}\right)^6\left(1 + \frac{N_B v_B}{N_A v_B}\right)^2\frac{v_B {l_C}^2}{v_C {l_B}^2}\frac{1}{S_2}\right\} \quad (23)$$

where

$$R_A^0 = 3^{1/3}\frac{(N_A v_A)^{2/3} {l_B}^{2/3}}{{v_B}^{1/3} {S_1}^{1/3}}\left(\frac{\gamma_{AB}}{kT}\right)^{1/3} \quad (24)$$

$$R_B^0 = 3^{1/3}\frac{(N_A v_A + N_B v_B)^{2/3} {l_C}^{2/3}}{{v_C}^{1/3} {S_2}^{1/3}} \times \left(\frac{\gamma_{BC}}{kT} + \frac{3}{10}\frac{1}{S_1}\frac{N_A v_A}{N_A v_A + N_B v_B}\frac{\gamma_{AB}}{kT}\right)^{1/3} \quad (25)$$

$$S_1 \equiv 1 + \frac{3\pi^2}{40}\frac{v_A {l_B}^2}{v_B {l_A}^2} \qquad S_2 \equiv 1 + \frac{1}{5}\frac{v_B {l_C}^2}{v_C {l_B}^2}$$

The radii R_A^0 and R_B^0 in the expressions 22−25 correspond to the radii of A-aggregates and the B-micelle for the case $R_A \ll R_B$ (i.e. for the case of many A-aggregates inside the B-micelle), respectively.

The analysis of the expressions 22 and 23 demonstrates that for the multi-A-aggregate case the radius of A-aggregates (and hence the aggregation number) becomes somewhat smaller than for the A−B-diblock copolymer case (R_{AB}). Simultaneously the radius (and aggregation number) of the B-micelle becomes larger than for the case when block *A* is identical to block B. Both of these effects can be explained from the following qualitative considerations. Since A-aggregates should be formed inside the finite space of the B-micelle, the size and the average distance between A-micelles change. Under the same value of surface tension coefficient (γ_{AB}) in infinite space, A-micelles can be packed less densely and as a result the radius R_{AB} is somewhat larger than R_A. Simultaneously the presence of A-aggregates inside the B-micelle core influences the size of the B-micelle. In the framework of electrostatic analogy, the A-aggregates act like identically charged small spheres. The repulsion of these spheres leads to the increase of the B-micelle size.

The aggregation numbers of A-aggregates and of the B-micelle as well as other parameter of the B-micelles structure can be easily calculated using the relations between these values and the radii of A-aggregates and the B-micelle (eqs 11 and 19). To avoid overcomplicating the paper, we do not present these expressions here. Another important characteristics of the B-micelle is the number of A-aggregates inside the core, *m*. This value can be obtained form the following simple calculation:

$$m \equiv \frac{Q_B}{Q_A} \sim \frac{(N_A v_A + N_B v_B)}{N_A v_A}\frac{v_B {l_C}^2}{v_C {l_B}^2}\frac{S_1}{S_2}\frac{\gamma_{BC}}{\gamma_{AB}} \times \left(1 + \frac{3}{10}\frac{N_A v_A}{N_A v_A + N_B v_B}\frac{\gamma_{AB}}{\gamma_{BC}}\right)$$

The condition $m = 1$ corresponds to the case when only one A-aggregate is present inside the core of the B-micelle. This condition is realized if

$$\frac{\gamma_{AB}}{kT} \sim \frac{(N_A v_A + N_B v_B)}{N_A v_A}\frac{\gamma_{BC}}{kT}\frac{v_B {l_C}^2}{v_C {l_B}^2}\frac{S_1}{S_2}\frac{1}{\left(1 - \frac{3}{10}\frac{v_B {l_C}^2}{v_C {l_B}^2}\frac{S_1}{S_2}\right)} \quad (26)$$

In the limit $m \to 1$, i.e. when condition 26 is fulfilled, the expressions 22 and 23 for the radii of A-aggregates and B-micelle are qualitatively similar to the expressions 16 and 18 obtained in the previous subsection for the case of a single A-aggregate at the center of the B-micelle

$$R_B \sim \text{const}\frac{(N_A v_A + N_B v_B)^{2/3} {l_C}^{2/3}}{{v_C}^{1/3} {S_2}^{1/3}}\left(\frac{\gamma_{BC}}{kT}\right)^{1/3}$$

$$R_A \sim \text{const}\frac{(N_A v_A)^{1/3}(N_A v_A + N_B v_B)^{1/3} {l_C}^{2/3}}{{v_C}^{1/3} {S_2}^{1/3}}\left(\frac{\gamma_{BC}}{kT}\right)^{1/3}$$

In the opposite limit, if $m \gg 1$, $R_A \simeq R_A^0$, $R_B \simeq R_B^0$. As we can see from eqs 22−25 for the case of many A-aggregates inside the B-micelle, the surface tension coefficient γ_{AB} is crucial for the formation of the satellite A-aggregates, while the coefficient γ_{BC} mainly influences the B-micelle formation, determining the size of the B-micelle.

The condition of superstrong segregation regime for A-aggregates for the multi-A-aggregate case is

$$\frac{\gamma_{AB}}{kT}\left\{1-\frac{3}{10}\frac{1}{S_1}\frac{R_A^0}{R_B^0}\left(1-\frac{8}{3}\left(\frac{R_A^0}{R_B^0}\right)^3\left(1+\frac{N_B v_B}{N_A v_B}\right)\right)\right\}^3 \geq \frac{N_A {l_A}^3 v_B}{{v_A}^2 {l_B}^2} S_1 \quad (27)$$

As it follows from the eq 27, if $m \to \infty$, the critical value of $\gamma_{AB}/(kT)$ is approximately the same as for A−B-diblock copolymers and is equal to

$$\left.\frac{\gamma_{AB}}{kT}\right|^{ss} \sim \frac{N_A {l_A}^3 v_B}{{v_A}^2 {l_B}^2} S_1$$

If $m \to 1$, the critical value of $\gamma_{AB}/(kT)$ defined by eq 27 tends to $(\gamma_{AB}/(kT))|^{ss}$ for the single A-aggregate case eq 20). For the intermediate values of m ($m \gg 1$) the critical value of $\gamma_{AB}/(kT)$ is somewhat larger than that for A−B-diblock copolymers. If inequality 27 is valid, A-aggregates should be disklike[32] (Figure 3b). B-micellar structure with disklike A-aggregates will be considered in detail in the next section.

4. Disklike A-Aggregates inside B-Micelle

In the present section we will consider structures of B-micelles which allow the presence of nonspherical A-aggregates. Following the result obtained in ref 32 that disklike aggregates are more preferable in the superstrong segregation limit, we will suppose that A-aggregates have a disklike form (Figure 3) with the diameter of the disk being D and the width being $H \equiv 2N_A l_A$ (see ref 32). We will consider the most interesting case, when $D \gg H$. Instead of the equations 11, connecting the size of the aggregate with its aggregation number, we will have then the following relation for A-aggregates:

$$Q_A = \frac{V_A}{N_A v_A} \simeq \frac{\pi}{2}\frac{{D_A}^2 l_A}{v_A} \quad (28)$$

where V_A and D_A are the volume and disk diameter of A-aggregates, respectively.

In section 2 the main ideas of the model were formulated for the case when the form of all A-aggregates is spherical. Now when we have to deal with nonspherical aggregates the main conclusions of section 2 have to be generalized. Thus, the expression for the free energy of the system of satellite A-aggregates (F^A) can be obtained in a similar way as in ref 32:

$$F^A = \left\{kT\frac{2}{\pi}\frac{v_B}{{l_B}^2}\frac{D_A l_A}{v_A} + \gamma_{AB}\left(\frac{v_A}{l_A}+\frac{\pi}{2}\frac{N_A v_A}{D_A}\right)\right\}\left(1-\frac{Q_0}{Q_B}\right) \quad (29)$$

The first term in the eq 29 corresponds to the free energy of the B-block extension near the surfaces of satellite A-aggregates. This expression can be obtained in the framework of an electrostatic analogy. Indeed, taking into account that the electrostatic energy of a thin disk ($D \gg H$) is

$$W = \frac{16}{3\pi}\frac{Q^2}{D}$$

(see, for instance, ref 34) we can define with help of eq 8 the free energy of B-block extension. The second term in eq 2 is the surface free energy of disklike A-aggregates.

Free energy of B-blocks extension in the core of the B-micelle (with the exception of the contribution already taken into account in eq 29) can be obtained using the electrostatic analogy in a similar way as for spherical aggregates (see the Appendix). The only difference is connected with the fact that for the present case we should consider the layer between the surface of the central aggregate, which is disklike, and the spherical surface of B-micelle. The free energy F^B has the form (eq A4 of the Appendix)

$$F^B \simeq kT\frac{3}{8\pi}\frac{v_B}{{l_B}^2}\left\{\frac{{Q_0}^2}{Q_B}\frac{2c}{D_0}+\frac{Q_0}{Q_B}\frac{(Q_B-Q_0)}{R_B}+\frac{1}{5}\frac{(Q_B-Q_0)^2}{Q_B R_B}\right\} \quad (30)$$

where $c = 16/(3\pi)$. (Here, as in the previous section, we will suppose that $D_0 \ll R_B$. This assumption is valid in the most of cases, but even if $D_0 \sim R_B$, our results remain qualitatively valid.) Expression 30 for the free energy F^B for the present case has a similar form as for the case of a spherical central aggregate (eq 9). As we can see, the last two terms in eqs 30 and 9 are identical, the difference arises only due to the contribution from the B-block extension near the surface of the central aggregate. It is clear that the extension of B-blocks near the surface of the disklike central aggregate is generally larger than near the spherical surface.

Now we can write the expression for full free energy without any assumptions about the size of the central disklike aggregate, as was done above. However, the free energy of the system with $Q_0 = Q_A$ again turns out to be lower than for the case $Q_0 \neq Q_A$. So, below we will present the results for the case $Q_0 = Q_A$. Thus the free energy of the system of B-micelles with identical disklike A-aggregates has the form

$$\frac{F}{kT} = \frac{2}{\pi}\frac{v_B}{{l_B}^2}\frac{D_A l_A}{v_A}+\frac{\gamma_{AB}}{kT}\left(\frac{v_A}{l_A}+\frac{\pi}{2}\frac{N_A v_A}{D_A}\right)+\frac{3}{16}\frac{{D_A}^2}{R_B}\frac{l_A v_B}{{v_A}{l_B}^2}\left[1-\frac{3}{8}\frac{{D_A}^2 l_A}{{R_B}^3 v_A}(N_B v_B+N_A v_A)\right]+\frac{1}{10}\frac{{R_B}^2 v_B}{(N_B v_B+N_A v_A){l_B}^2}\left[1-\frac{3}{8}\frac{{D_A}^2 l_A}{{R_B}^3 v_A}(N_B v_B+N_A v_A)\right]^2+3\frac{(N_B v_B+N_A v_A)}{R_B}\frac{\gamma_{BC}}{kT}+\frac{1}{2}\frac{{R_B}^2 v_C}{(N_B v_B+N_A v_A){l_C}^2} \quad (31)$$

As in the previous section, let us start our consideration with the case of a single aggregate at the center of the B-micelle.

4.1. Single Disklike Aggregate at the Center of the B-Micelle. As it has been mentioned in subsection 3.1, when the value of $\gamma_{eff}(kT)$ (eq 15) becomes larger than $(N_A {l_A}^3 v_B)/({v_A}^2 {l_B}^2)S$, the form of the central aggregate cannot stay spherical because of the volume (or surface) restrictions. Then the central aggregate should transform to a disklike shape (Figure 3a). If a single A-aggregate is present at the center of the B-micelle,

the variables D_A and R_B are not independent and are connected via the following volume relation:

$$D_A = \sqrt{\frac{8}{3}\frac{{R_B}^3 v_A}{(N_B v_B + N_A v_A) l_A}}$$

Taking into account this relation we can rewrite the expression for the free energy (eq 31) in the form

$$\frac{F}{kT} = \frac{2}{\pi}\frac{v_B}{{l_B}^2}\frac{D_A l_A}{v_A} + \frac{\gamma_{AB}}{kT}\left(\frac{v_A}{l_A} + \frac{\pi}{2}\frac{N_A v_A}{D_A}\right) + 3\left(\frac{8}{3}\right)^{1/3}\frac{(N_B v_B + N_A v_A)^{2/3} {v_A}^{1/3}}{D^{2/3} {l_A}^{1/3}}\frac{\gamma_{BC}}{kT} + \frac{1}{2}\left(\frac{3}{8}\right)^{2/3}\frac{{D_A}^{4/3} {l_A}^{2/3} v_C}{(N_B v_B + N_A v_A)^{1/3} {l_C}^2 {v_A}^{2/3}} \quad (32)$$

Minimization of the free energy (eq 32) allows determination of the equilibrium structural parameters of the A-aggregate and B-micelle:

$$D_A \simeq \frac{{N_A}^{1/2} v_A l_B}{{v_B}^{1/2} {l_A}^{1/2}} \times \left\{\frac{\gamma_{AB}}{kT} + \frac{{l_B}^{2/5}(N_B v_B + N_A v_A)^{4/5}}{{l_A}^{3/5} {v_B}^{1/5} N_A {v_A}^{2/5}}\left(\frac{\gamma_{BC}}{kT}\right)^{6/5}\right\}^{1/2} \quad (33)$$

$$R_B \simeq \frac{{N_A}^{1/3} {v_A}^{1/3} {l_B}^{2/3}}{{v_B}^{1/3}}(N_B v_B + N_A v_A)^{1/3} \times \left\{\frac{\gamma_{AB}}{kT} + \frac{{l_B}^{2/5}(N_B v_B + N_A v_A)^{4/5}}{{l_A}^{3/5} {v_B}^{1/5} N_A {v_A}^{2/5}}\left(\frac{\gamma_{BC}}{kT}\right)^{6/5}\right\}^{1/3} \quad (34)$$

$$Q \simeq \frac{N_A v_A {l_B}^2}{v_B}\left\{\frac{\gamma_{AB}}{kT} + \frac{{l_B}^{2/5}(N_B v_B + N_A v_A)^{4/5}}{{l_A}^{3/5} {v_B}^{1/5} N_A {v_A}^{2/5}}\left(\frac{\gamma_{BC}}{kT}\right)^{6/5}\right\}$$

$$\lambda_B \simeq (Q N_C v_C)^{1/3} \simeq \left[N_C v_C \frac{N_A v_A {l_B}^2}{v_B} \times \left\{\frac{\gamma_{AB}}{kT} + \frac{{l_B}^{2/5}(N_B v_B + N_A v_A)^{4/5}}{{l_A}^{3/5} {v_B}^{1/5} N_A {v_A}^{2/5}}\left(\frac{\gamma_{BC}}{kT}\right)^{6/5}\right\}\right]^{1/3}$$

As for the case of a single central spherical A-aggregate (eqs 16−18 and 19), the size of A-aggregates is larger than for the A−B-diblock copolymers, and simultaneously the size of the B-micelle is smaller than for the case when the A-block is identical to the B-block. The explanation of this effect is similar to that for a spherical central A-aggregate. The larger the radius of the B-micelle is, the more stretched the B-block inside the micelle is. The extension of the B-chains inside the core in the presence of the A-aggregate is larger than for the reference diblock copolymer case since all B-chains have to terminate near the center of the B-micelle. As a result, to reduce the extension of B-chains, the equilibrium size of B-micelle decreases.

Our calculations have been performed using the assumption that the diameter of the disks (D_A) is much smaller than the radius of the B-micelle, i.e. if $D_A \ll 2R_B$. This condition leads to the following inequality

$$\frac{\gamma_{AB}}{kT} + \frac{{l_B}^{2/5}(N_B v_B + N_A v_A)^{4/5}}{{l_A}^{3/5} {v_B}^{1/5} N_A {v_A}^{2/5}}\left(\frac{\gamma_{BC}}{kT}\right)^{6/5} \le \frac{(N_B v_B + N_A v_A)^2 v_B {l_A}^3}{{l_B}^2 {v_A}^4 N_A} \quad (35)$$

which is probably always valid for real polymer systems. Indeed, this inequality can be violated only for extremely large values of surface tension coefficients; for instance, if

$$\frac{\gamma_{AB}}{kT} > \frac{(N_B v_B + N_A v_A)^2 v_B {l_A}^3}{{l_B}^2 {v_A}^4 N_A}$$

or if

$$\frac{\gamma_{BC}}{kT} \ge \frac{(N_B v_B + N_A v_A) v_B {l_A}^3}{{l_B}^2 {v_A}^3}$$

that does not correspond to real conditions.

Several Disklike A-Aggregates inside the B-Micelle. In this section we will consider the case when there are several disklike A-aggregates inside the B-micelle (Figure 3b), i.e. $Q_B \neq Q_A$. To determine the diameter and aggregation number of A-aggregates as well as the size and aggregation number of the B-micelle, we have to minimize the free energy (eq 31) with respect to the independent variables D_A and R_B. The following are the results of the calculations

$$D_A \simeq D_A^0\left\{1 - \frac{\pi}{2}\frac{9}{80}\frac{D_A^0}{R_B^0}\left(1 - \frac{(D_A^0)^2 l_A}{(R_B^0)^3 v_A}(N_B v_B + N_A v_A)\right)\right\} \quad (36)$$

$$R_B \simeq R_B^0\left\{1 - \frac{3}{40}\frac{(D_A^0)^4 {l_A}^2}{(R_B^0)^6 {v_A}^2}(N_B v_B + N_A v_A)^2 \frac{v_B {l_C}^2}{v_C {l_B}^2}\frac{1}{S_2}\right\} \quad (37)$$

where

$$D_A^0 \simeq \frac{\pi}{2}\frac{{N_A}^{1/2} v_A l_B}{{v_B}^{1/2} {l_A}^{1/2}}\left(\frac{\gamma_{AB}}{kT}\right)^{1/2} \quad (38)$$

$$R_B^0 \simeq 3^{1/3}\frac{(N_A v_A + N_B v_B)^{2/3} {l_C}^{2/3}}{{v_C}^{1/3} {S_2}^{1/3}} \times \left(\frac{\gamma_{BC}}{kT} + \frac{3}{80}\frac{\pi^2}{4}\frac{N_A v_A}{N_A v_A + N_B v_B}\frac{\gamma_{AB}}{kT}\right)^{1/3} \quad (39)$$

$$S_2 \equiv 1 + \frac{1}{5}\frac{v_B {l_C}^2}{v_C {l_B}^2}$$

In a similar way as for the case of spherical A-aggregates considered in the previous section, the expressions 38 and 39 for the A-aggregate diameter (D_A^0) and the radius of B-micelle (R_B^0) correspond to the case $R_B \gg D_A$. In this case there are many ($m \gg 1$) A-aggregates inside the B-micelle. The main tendencies of the behavior of these values are similar to the case of spherical aggregates. Moreover, the expression for

the radius of a B-micelle differs from that for the case of spherical aggregates only in the numerical coefficient. Thus, the radius of a B-micelle remains larger than for the case where the A-block is identical to the B-block. The diameter of the A-aggregate is generally larger than for the A−B-diblock copolymer case. The explanation of these effects is identical to that for the case of spherical aggregates.

One of the common features of behavior of polymer micelles with several aggregates inside is that the size of the B-aggregate is substantially larger than that for the micelles with a single A-aggregate. The physical reason for this effect is clear enough. Indeed, if there are several A-aggregates inside a B-micelle, B-blocks can terminate not only at the center of B-micelle but also in the satellite A-aggregates. It is thus evident that the extension of B-chains in the case of several A-aggregates is smaller than for the single A-aggregate case. As a result, the size of the B-micelle for the case of several A-aggregates ($m \gg 1$) is much larger.

As for the case of spherical A-aggregates, we do not present the expressions for aggregation numbers and other parameters of the B-micelle, as they can be easily obtained using eqs 11, 28, and 19. The number of satellite A-aggregates inside the B-micellar core is approximately the same for spherical and disklike satellite aggregates cases:

$$m \equiv \frac{Q_B}{Q_A} \simeq \frac{32}{\pi^2}\frac{(N_A v_A + N_B v_B)}{N_A v_A}\frac{v_B {l_C}^2}{v_C {l_B}^2}\frac{1}{S_2}\frac{\gamma_{BC}}{\gamma_{AB}} \times \left(1 + \frac{3}{80}\frac{\pi^2}{4}\frac{N_A v_A}{N_A v_A + N_B v_B}\frac{\gamma_{AB}}{\gamma_{BC}}\right)$$

As for the case of spherical A-aggregates, in the limit $m \to 1$, i.e. if

$$\frac{\gamma_{AB}}{kT} \sim \frac{(N_A v_A + N_B v_B)}{N_A v_A}\frac{\gamma_{BC}}{kT}\frac{v_B {l_C}^2}{v_C {l_B}^2}\frac{1}{S_2}\frac{1}{\left(1 - \frac{3}{10}\frac{v_B {l_C}^2}{v_C {l_B}^2}\frac{1}{S_2}\right)}$$

the expressions for the radius of the B-micelle and the diameter of A-aggregates (eqs 36 and 37) are qualitatively similar to that for the case of a single disklike A-aggregate (eqs 33 and 34).

In the present and in the previous sections we have considered the possible configurations of the inner structure of the B-micelle core. The next step of our analysis is to define the conditions of stability of one or another type of micelle. The full picture of different regimes of behavior of the system under consideration will be discussed in the next section.

5. Different Types of the Inner Structure of the B-Micelle

First of all, let us obtain the conditions of validity of our approach. Since the calculations have been performed in the framework of a strong segregation limit, we should define the conditions for the realization of this regime. In the strong segregation limit, the boundaries between different domains are sharp. This means that the typical free energy per block should be large enough: $F/(kT) \gg 1$. This inequality leads to the following condition of the strong segregation regime for the present polymer system:

$$\frac{\gamma_{BC}}{kT} + \frac{3}{10}\frac{1}{S_1}\frac{N_A v_A}{N_A v_A + N_B v_B}\frac{\gamma_{AB}}{kT} \gg \frac{l_C}{(N_A v_A + N_B v_B)^{1/2} {v_C}^{1/2} {S_2}^{1/2}} \times \left[1 - \frac{3}{2}\frac{3^{2/3} {S_1}^{1/3} (N_A v_A)^{1/3} {v_B}^{1/3}}{{l_B}^{2/3}}\left(\frac{\gamma_{AB}}{kT}\right)^{2/3}\right]^{3/2} \quad (40)$$

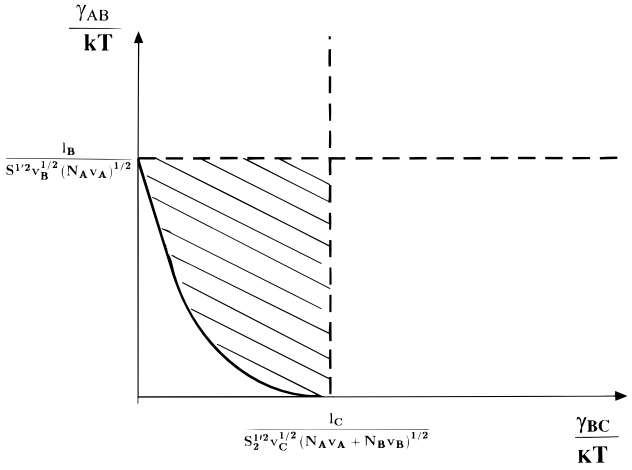

Figure 4. Diagram showing the boundary of strong segregation for the polymer system. The dotted lines correspond to the boundaries of the region of strong segregation regimes for A−B- and B−C-block copolymers. The shaded region is the region of strong segregation, which is easier to realize for the present polymer system than for the corresponding diblock copolymer systems.

In Figure 4 the boundary of the strong segregation limit for the polymer system is shown. As is seen from Figure 4, the strong segregation limit can be reached for surface tension coefficients γ_{AB} and γ_{BC} which are smaller than the critical values of $\gamma_{AB}S$ and $\gamma_{BC}S$ for strong segregation regime for the corresponding A−B- and B−C-block copolymer micelles. The dotted vertical line $\gamma_{BC} = \gamma_{BC}^S = l_C/[(N_A v_A + N_B v_B)^{1/2}\, v_C^{1/2}$, and the horizontal line, $\gamma_{AB} = \gamma_{AB}^S = l_B/(N_A v_A v_B)^{1/2}$, mark the regions of the strong segregation regime for the corresponding diblock copolymer micelles. As we can see from Figure 4, for A−B−C-block copolymer micelles, the strong segregation regime can be realized for conditions where neither A−B- nor B−C-diblock copolymer systems correspond to the strong segregation (shaded regions in Figure 4). So, the presence of the A-aggregates inside the core of the B-micelle enhances the microphase separation tendency and stabilizes the B-micelle structure.

In the previous sections we considered two principally different types of micelles: (i) with single (spherical or disklike) A-aggregate at the center of the B-micelle and (ii) with several (spherical or disklike) A-aggregates inside the B-micelle. It is natural to expect that the first type of structures can be realized when the incompatibility of A−B-blocks is much larger than that of B−C-blocks, i.e. if $\gamma_{AB} \gg \gamma_{BC}$. Indeed, a comparison of the free energies of B-micelles with spherical A-aggregates inside demonstrates that, for relatively large γ_{AB}, polymer micelles with a single A-aggregate are

more favorable:

$$\frac{\gamma_{BC}}{kT}\left(1-\left(\frac{N_A v_A}{N_A v_A + N_B v_B}\right)^{1/3}\right) \sim \frac{\gamma_{AB}}{kT}\frac{N_A v_A}{N_A v_A + N_B v_B}\frac{1}{S}\left(\frac{9}{4}+\frac{v_C l_B^2}{v_B l_C^2}\right) \quad (41)$$

Similar calculations performed for other types of micelles lead us to the following results. If

$$\frac{\gamma_{BC}}{kT}\left(1-\left(\frac{\frac{\gamma_{BC}}{kT}}{N_A v_A + N_B v_B}\right)^{1/5}\right) \le \frac{\gamma_{AB}}{kT}\frac{N_A v_A}{N_A v_A + N_B v_B}\left(\frac{9}{4}+\frac{1}{2}\frac{v_C l_B^2}{v_B l_C^2}\right) \quad (42)$$

polymer micelles with single disklike A-aggregate are formed in the polymer system. As we can see, the main tendency to form the polymer system with a single A-aggregate for sufficiently large surface tension coefficients γ_{AB} is unchanged for the superstrong segregation limit for A-aggregates. As has been mentioned above, the superstrong segregation regime is more easily reached for the single A-aggregate case than for the A−B-diblock copolymer case. Indeed, the boundary condition for the superstrong segregation limit is defined by eq 20

$$\left(\frac{\gamma_{AB}}{kT}+\left(1+\frac{N_B v_B}{N_A v_A}\right)^{2/3}\frac{\gamma_{BC}}{kT}\right)\Bigg|_{ss} \ge \frac{N_A l_A^3 v_B}{v_A^2 l_B^2} S$$

If $\gamma_{BC} = 0$, this is in fact the condition of the superstrong segregation regime for the diblock copolymer case. So, the presence of a C-block that is incompatible with B-units promotes the superstrong segregation regime for A−B microsegregation. As a result, for triblock copolymer systems, the single A-aggregate inside the B-micelle can be in the superstrong segregation regime, even if the reference diblock copolymer A-aggregate is in the strong segregation regime.

For the multi-A-aggregate case ($m \gg 1$) the size of A-aggregates is somewhat smaller than for the A−B-diblock copolymer case. Hence, the boundary of the superstrong segregation regime is reached for somewhat larger surface tension coefficients:

$$\frac{\gamma_{AB}}{kT}\left\{1-\frac{3}{10}\left(\frac{N_A v_A}{N_A v_A + N_B v_B}\right)^{2/3}\frac{v_C^{1/3} l_B^{2/3}}{v_B^{1/3} l_C^{2/3}}\frac{S_2^{1/3}}{S_1^{4/3}}\left(\frac{\gamma_{AB}}{\gamma_{BC}}\right)^{1/3} \times \left(1-\frac{8}{3}\frac{N_A v_A}{N_A v_A + N_B v_B}\frac{v_C l_B^2}{v_B l_C^2}\frac{S_2}{S_1}\frac{\gamma_{AB}}{\gamma_{BC}}\right)\right\} \ge \frac{N_A l_A^3 v_B}{v_A^2 l_B^2} S_1 \quad (43)$$

For $m \to \infty$, this condition is transformed to the superstrong segregation condition for A−B-diblock copolymers,

$$\frac{\gamma_{AB}}{kT} \ge \frac{N_A l_A^3 v_B}{v_A^2 l_B^2} S_1$$

This limit corresponds to the case when the size of the B-micelle is very large, so the presence of the surface of the B-micelle does not influence significantly the formation of the A-aggregates. If $m \to 1$, i.e if there is only one A-aggregate at the center of B-micelle, the critical value of $\gamma_{AB}/(kT)$ coincides with that obtained in subsection 3.1 (eq 20).

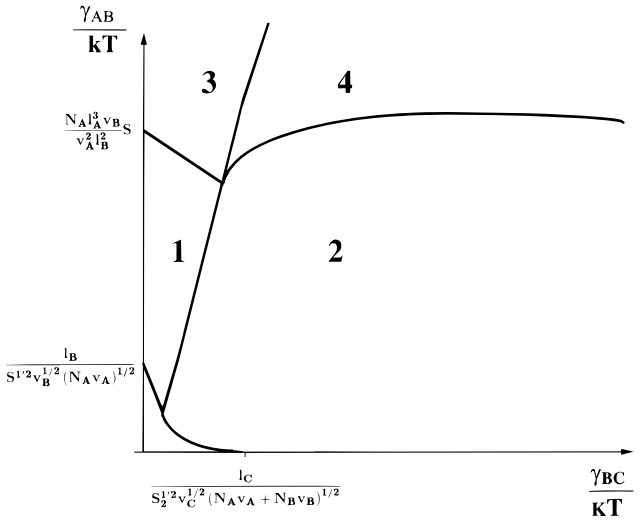

Figure 5. Diagram of different regimes for a B-micelle. The diagram contains regions of the B-micelle with a single spherical aggregate (region 1), several spherical A-aggregates (region 2), a single disklike aggregate (region 3), and several disklike A-aggregates (region 4).

Now we have all boundary conditions for the construction of the diagram of states for the spherical B-micelles. In Figure 5 four different types of B-micelles are represented. The diagram is plotted in the variables $\gamma_{AB}/(kT)$ and $\gamma_{BC}/(kT)$. Region 1 corresponds to the case of a single spherical A-aggregate at the center of the micelle. Region 3 is also the region of the micelle with a single A-aggregate at the center, but the form of this aggregate is disklike. The boundary between regions 1 and 3 is the boundary of the superstrong segregation regime for the central A-aggregate. It is defined by eq 20. Regions 2 and 4 correspond to multi-A-aggregate micelles with spherical and disklike aggregates, respectively. The boundary between these regions is defined by condition 43, which is the condition of the superstrong segregation regime for A-aggregates. The regions corresponding to a single A-aggregate micelles and multi-A-aggregate micelles are separated by the curves defined by the conditions 41 and 42. The curve cutting off the lower left corner of the diagram corresponds to the condition of strong segregation for the polymer system (40). Our results are valid in the regions above this curve.

The main characteristics of different types of polymer micelles were calculated in the previous sections. As we have seen, the radii and aggregation numbers of micelles strongly depend on the lengths of the blocks, their incompatibility, and monomer unit parameters. As a result, the diagram of states also depends on these values. For instance, the increase of block length N_A leads to the expansion of the regions of B-micelles with a single A-aggregate inside. However, the qualitative form of the phase diagram is always the same and corresponds to Figure 5.

6. Conclusion

We have considered different types of B-micellar structure for the A−B−C-triblock copolymer melts with $N_A + N_B \ll N_C$. We have restricted our analysis to the case of the spherical form of B-micelles. As we have seen, the incompatibility of blocks and the presence of the short A-block at the end of the B-block leads to the formation of B-micelles with a complicated inner struc-

ture. In all the regimes there is an A-aggregate at the center of the micelle. This can be either the single A-aggregate or the element of the system of several A-aggregates.

As has been shown, the presence of the A-aggregates inside the core of the B-micelle shifts the boundary of the strong segregation regime to smaller values of surface tension coefficients γ_{AB} and γ_{BC} (Flory−Huggins parameters) in comparison with A−B- or B−C-diblock copolymer cases. Indeed, the following situation can take place: triblock copolymer micelles are in a strong segregation regime, while the reference diblock copolymer system corresponds to weak segregation, or even no microaggregation at all. This means that the presence of A-blocks enhances microphase separation. This conclusion is in agreement with experimental results.[10]

Depending on the values of surface tension coefficients, the form of the A-aggregates can be different. For relatively low values of γ_{AB}, the A-aggregates have a spherical form, while for large values of γ_{AB}, in the superstrong segregation regime, they are disklike.[32] For the single A-aggregate case the size of the A-aggregate is somewhat larger than that for the A−B-diblock copolymer case. As a result, for this case the superstrong segregation regime is reached for smaller values of the surface tension coefficients than for the A−B-diblock copolymer. So, for a triblock copolymer system, not only the strong segregation regime but also the superstrong segregation limit is reached much more easily than for the corresponding diblock copolymer systems. The presence of A-blocks inside the core of a B-micelle intensifies the segregation tendency between B- and C-blocks. Simultaneously, the presence of a C-block stimulates segregation between A- and B-blocks for the single A-aggregate case.

There are four different regimes for the B-micelle structure shown in Figure 5. The main tendency connected with the B-micelles is the following. If the A−B-interaction parameter χ_{AB} (γ_{AB}) is much larger than χ_{BC} (γ_{BC}), the B-micelles are formed in such a way as to ensure the existence of a single A-aggregate in the center of these micelles. In the opposite case, when the main restrictions are imposed by the B−C-incompatibility, the multi-A-aggregate structure of the B-micelle core is realized. For the case of a single A-aggregate per B-micelle, the size (aggregation number) of the B-micelle is smaller than that for the B−C-diblock copolymer case (when block *A* is identical to block B). On the other hand, the size of a B-micelle with several A-aggregates inside is larger than the size of a B−C-diblock copolymer micelle (and much larger than the size of a B-micelle with a single A-aggregate).

The comparison of the present results with the experimental data of ref 10 leads to the conclusion that most probably for those polymer systems polymer micelles with a single A-aggregate at the center of a B-micelle are present. Indeed, since the ω-functionalized groups are strongly interacting ones, this interaction is much stronger than the repulsion between PS−PI-blocks and plays the dominant role in the behavior of the system. In terms of the present model, $\gamma_{AB} \gg \gamma_{BC}$. As has been mentioned above for this case, it may be favorable to form the polymer micelle with a single A-aggregate at the center. However, the relation between the block lengths should be taken into account as well. For the polymer system of ref 10, $N_A \sim 1$, $N_B/N_C \sim 0.33$. Since the present analysis deals only with the case of spherical B-micelles ($N_A + N_B \ll N_C$), the experimental data of ref 10 (cylindrical micelles) cannot be exactly interpreted in the framework of our theory. Generalizing our results for this case, we can expect that the micelles with a single A-aggregate or with several A-aggregates will be formed depending on the parameters in the system. But even for multi-A-aggregate micelles, the number of A-aggregates inside the B-micelle for the case of ref 10 is not expected to be large. Thus, the size of the B-micelle should be either smaller than for the B−C-copolymer case (that is, in agreement with the data of the SAXS measurements[10]) or comparable with the size of the reference diblock copolymer.

It is worthwhile also to comment on the temperature dependencies of all the calculated parameters. All characteristics of the B-micelle depend on the surface tension coefficients, which are connected with the interaction parameters of monomer units (see eq 3) and hence with the temperature. So, the exact dependence of calculated parameters on temperature can be rather complicated. As a zero-order approximation, we can consider surface tension coefficients to be temperature independent. For this case the dependence of the calculated parameters on temperature follows directly from equations written above. Thus, the radius of the B-micelle and the average distance between micelles (as well as other characteristics) should decrease as the temperature increases. This is also in qualitative accord with ref 10.

Acknowledgment. The authors are grateful to Dr. G. Floudas and Prof. G. Ten Brinke for valuable comments. They also thank the Russian Foundation for Fundamental Research for financial support.

Appendix

The Calculation of the Free Energy of B-Block Extension in the Framework of the Electrostatic Analogy. The electrostatic analogy[7,32] is based on the fact that the conformation of polymer chains near the surface of a micelle is similar to the electric field lines near charged surfaces. Let us denote by $r(n)$ the average distance of the nth monomer unit of the B-block from the surface of the central A-aggregate. In the framework of the electrostatic analogy, the average vector connecting neighboring monomer units along the chain dr/dn corresponds to the electric field, E, the aggregation numbers are associated with the electric charges. To obtain the free energy of the B-block extension (F^B) in the spherical layer between the surface of the central aggregate and the surface of the B-micelle, we must define the "electric field" in this region. We know that the "charge" of the central aggregate is equal to Q_0, while the joint "charge" of the B-micelle is Q_B. Between these surfaces there are satellite "charges", Q_A. To calculate the "electric field" of this system of "charges", we need to know the distribution of satellite "charges" inside the core. It is necessary to emphasize that the free energy of B-block extension is of an entropic nature. The smaller the distance between the ends of the B-block, the more conformations that are available for this block. So, it is more important at which distance from the surface of the micelle the B-block is terminated than to which satellite A-aggregate it belongs. On the basis of these considerations, we will neglect the discrete nature of A-aggregates and assume that they are on average uniformly distributed inside the layer for the calculation of F^B. The average density of the "electric charge" inside the layer is

$$\frac{3}{4\pi}\frac{Q_B - Q_0}{R_B^3 - R_0^3}$$

We can also introduce the "joint charge" $Q(r)$ of the sphere of radius r:

$$Q(r) = Q_0 + \frac{Q_B - Q_0}{R_B^3 - R_0^3} r^3 \quad \text{(A1)}$$

The "electric field" in the layer can be represented in the form

$$E = \frac{Q(r)}{r^2}$$

Near the surface of the central aggregate ($r = R_0$) the "electric field" tends toward Q_0/r^2; near the surface of the B-micelle ($r = R_B$) it is about Q_B/r^2.

In the framework of the electrostatic analogy, the free energy of the B-blocks extension is proportional to the electrostatic energy $W = 1/(8\pi)\int E^2 \, d^3r$

$$F^B = kT \frac{1}{Q_B} CW = kT \frac{1}{Q_B} C \frac{1}{8\pi} \int E^2 \, d^3r \quad \text{(A2)}$$

where C is the polymer/electrostatic proportionality constant[32]

$$C = \frac{3}{4\pi} \frac{v_B}{l_B^2}$$

The calculation of the integral (A2) over the volume of the spherical layer allows us to obtain the free energy of B-block extension in this region

$$F^B \simeq kT \frac{3}{8\pi} \frac{v_B}{l_B^2} \left\{ \frac{Q_0^2}{Q_B} \frac{1}{R_0} + \frac{Q_0}{Q_B} \frac{(Q_B - Q_0)}{R_B} + \frac{1}{5} \frac{(Q_B - Q_0)^2}{Q_B R_B} \right\} \quad \text{(A3)}$$

The expression for the free energy (A3) was written taking into account the natural assumption that the radius of the central aggregate (R_0) is much smaller than the radius of the B-micelle (R_B), i.e. $R_0 \ll R_B$. However, even if we imagine that these values are comparable ($R_0 \sim R_B$), this can change some numerical coefficients, but all principal dependencies remain the same.

For the disklike form of A-aggregates, the free energy for B-block extension can be calculated in the similar way. It is only necessary to take into account that the form of the central aggregate is disklike, so the expression for "joint charge" (eq A1) takes the form

$$Q(r) = Q_0 + \frac{Q_B - Q_0}{R_B^3 - \frac{3}{8} D_0^2 N_A l_A} r^3$$

Taking the integral (A2) over the layer between the disklike central aggregate and spherical surface of the B-micelle, we obtain the free energy of B-block expansion

$$F^B \simeq kT \frac{3}{8\pi} \frac{v_B}{l_B^2} \left\{ \frac{Q_0^2}{Q_B} \frac{2c}{D_0} + \frac{Q_0}{Q_B} \frac{(Q_B - Q_0)}{R_B} + \frac{1}{5} \frac{(Q_B - Q_0)^2}{Q_B R_B} \right\} \quad \text{(A4)}$$

where $c = 16/(3\pi)$.

In the limit $Q_B \rightarrow Q_0$, the free energy (A4) tends to that for B-block extension near the disklike surface (the corresponding "electrostatic energy" is the energy of a thin disk[34]).

References and Notes

(1) Meier, D. J. *J. Polymer Sci. Part C* **1969**, *26*, 81.
(2) Helfand, E. *Macromolecules* **1975**, *8*, 552.
(3) Helfand, E.; Wasserman, Z. R. *Macromolecules* **1978**, *11*, 960.
(4) Goodman, I., Ed. *Developments in Block Copolymers*; Applied Science: New York, 1982; Vol. 1; 1985; Vol. 2.
(5) Erukhimovich, I. Ya.; *Vysokomol. Soedin.* **1982**, *24A*, 1942; (*Polym. Sci. USSR* **1983**, *24*, 2223).
(6) Leibler, L. *Macromolecules* **1980**, *13*, 1602.
(7) Semenov, A. N. *Sov. Phys. JETP* **1985**, *61*, 733.
(8) Ohta, T.; Kawasaki, K. *Macromolecules* **1986**, *19*, 2621.
(9) Fredrickson, G. H.; Helfand, E. *J. Chem. Phys.* **1987**, *87*, 697.
(10) Floudas, G.; Fytas, G.; Pispas, S.; Hadjichristidis, N.; Pakula, T.; Khokhlov, A. R. *Macromolecules* **1995**, *28*, 5109.
(11) Zhou, Z.; Chu, B. *Macromolecules* **1988**, *21*, 2548.
(12) Plestil, J.; Hlavata, D.; Hrouz, J.; Tuzar, Z. *Polymer* **1990**, *31*, 2112.
(13) Auschra, C.; Stadler, R. *Macromolecules* **1993**, *26*, 2171.
(14) Auschra, C.; Stadler, R. *Macromolecules* **1993**, *26*, 6364.
(15) Zhou, Z.; Chu, B. *Macromolecules* **1994**, *27*, 2025.
(16) Alexandridis, P.; Holtzwarth, J. F.; Hatton, T. A. *Macromolecules* **1994**, *27*, 2414.
(17) Mogi, Y.; Nomura, M.; Kotsuji, H.; Ohnishi, K.; Matsushita, Y.; Noda, I. *Macromolecules* **1994**, *27*, 6755.
(18) Krappe, U.; Stadler, R.; Voigt-Martin, I. *Macromolecules* **1995**, *28*, 4558.
(19) Almgren, M.; Brown, W.; Hvidt, S. *Colloid Polym. Sci.* **1995**, *273*, 2.
(20) Stadler, R.; Auschra, C.; Beckmann, J.; Krappe, U.; Voight-Martin, I.; Leibler, L. *Macromolecules* **1995**, *28*, 3080.
(21) Lyatskaya, Yu. V.; Birshtein, T. M. *Polymer* **1995**, *36*, 975.
(22) Nakazawa, H.; Ohta, T. *Macromolecules* **1993**, *26*, 5503.
(23) Zheng, W.; Wang, Z.-G. *Macromolecules* **1995**, *28*, 7215.
(24) Erukhimovich, I. Ya.; et al., manuscript in preparation.
(25) Eisenberg, A. *Macromolecules* **1970**, *3*, 147.
(26) Eisenberg, A.; King, M. *Ion-Containing Polymers*; Academic Press: New York, 1977.
(27) Eisenberg, A.; Hird, B.; Moore, M. *Macromolecules* **1990**, *23*, 4098.
(28) Kim, J.-S.; Jackman, J.; Eisenberg, A. *Macromolecules* **1994**, *27*, 2789.
(29) Yarusso, D. J.; Cooper, S. L. *Macromolecues* **1983**, *16*, 1871.
(30) Yarusso, D. J.; Cooper, S. L. *Polymer* **1985**, *26*, 371.
(31) Nyrkova, I. A.; Khokhlov, A. R.; Doi, M. *Macromolecules* **1993**, *26*, 3601.
(32) Semenov, A. N.; Nyrkova, I. A.; Khokhlov, A. R. *Macromolecules* **1995**, *28*, 7491.
(33) Semenov, A. N.; Nyrkova, I. A.; Khokhlov, A. R. Statistics and Dynamics of Ionomer Systems. In: *Ionomers: Properties and Applications*; Schlick, S., Ed., 1996; p 251.
(34) Landau L. D., Lifshitz E. M. *Electrodynamics of Continuous Media*; Pergamon Press: Oxford, U.K., 1984.

MA961076B